

Uplift and Seismicity Driven by Groundwater Depletion in Central California

C. Amos¹, P. Audet², W. Hammond³, R. Bürgmann^{4,5}, I. Johanson⁴, G. Blewitt³

¹Department of Geology, Western Washington University

²Department of Earth Sciences, University of Ottawa

³Nevada Geodetic Laboratory, Nevada Bureau of Mines and Geology, and Nevada Seismological Laboratory, University of Nevada, Reno

⁴Berkeley Seismological Laboratory, University of California, Berkeley

⁵Department of Earth & Planetary Science, University of California, Berkeley

1. Abstract

Groundwater use in California's San Joaquin Valley exceeds replenishment of the aquifer, leading to substantial diminution of this resource and rapid subsidence of the valley floor. The volume of groundwater lost over the past century-and-a-half also represents a substantial reduction in mass and a large-scale unburdening of the lithosphere, with significant but unexplored potential impacts on crustal deformation and seismicity. Here we use vertical GPS measurements to show that a broad zone of rock uplift up to $1 - 3 \text{ mm yr}^{-1}$ surrounds the southern San Joaquin Valley. The observed uplift matches well with predicted flexure from a simple elastic model of current rates of water-storage loss, the majority of which is caused by groundwater depletion. Height of the adjacent central Coast Ranges and Sierra Nevada is strongly seasonal and peaks during the dry late summer and fall, out of phase with inflation of the valley floor during wetter months. Our results suggest that long-term and late-summer flexural uplift of the Coast Ranges reduce the effective normal stress resolved on the San Andreas Fault. This process brings the fault closer to failure, thereby providing a viable mechanism for observed seasonality in microseismicity at Parkfield and potentially affecting long-term seismicity rates for fault systems adjacent to the valley. We also infer that observed contemporary uplift of the southern Sierra Nevada previously attributed to tectonic and/or mantle derived forces is partly a consequence of human-caused groundwater depletion.

2. Vertical GPS Data

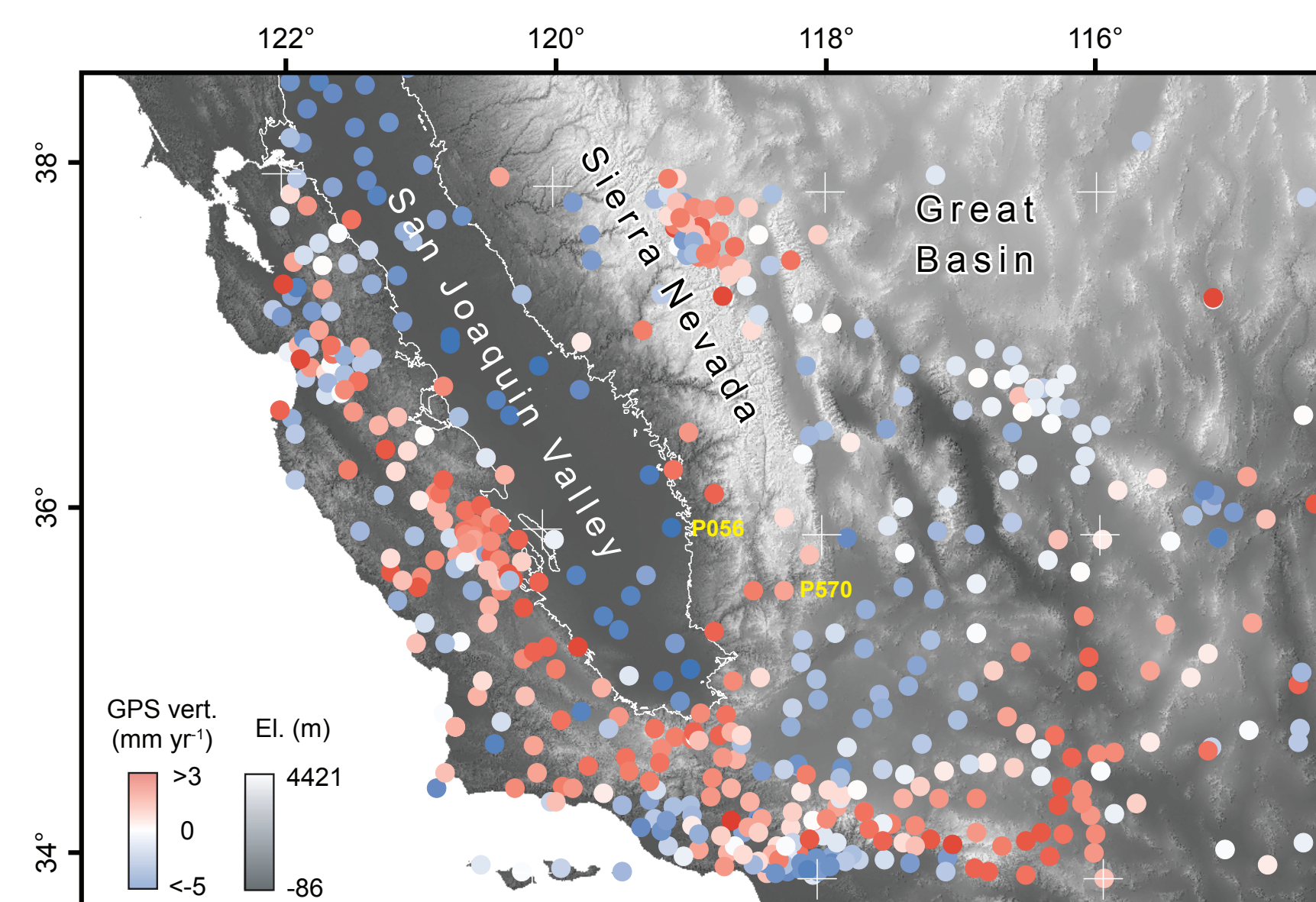
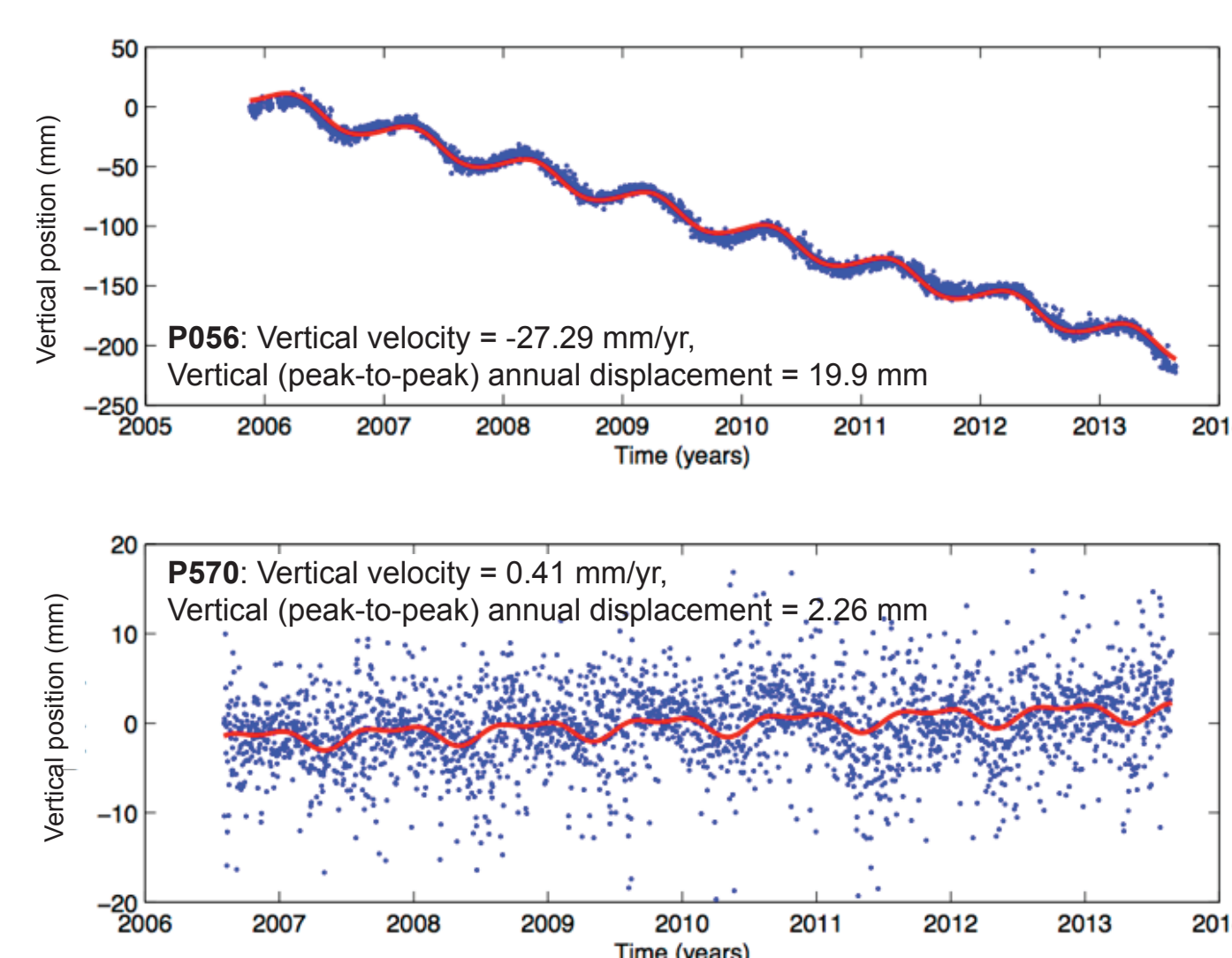


Figure 1. | Vertical GPS data

Map of vertical uplift rates spanning California and the western Great Basin from continuous and semi-continuous GPS stations.

Figure 2. | Example vertical GPS time series.

Blue dots are daily vertical position solutions, red lines are the model estimated to represent the time series. The station P056 is in the southern Central Valley near Porterville, CA. The station P570 is near Weldon, CA east of Lake Isabella.



3. Groundwater Loss

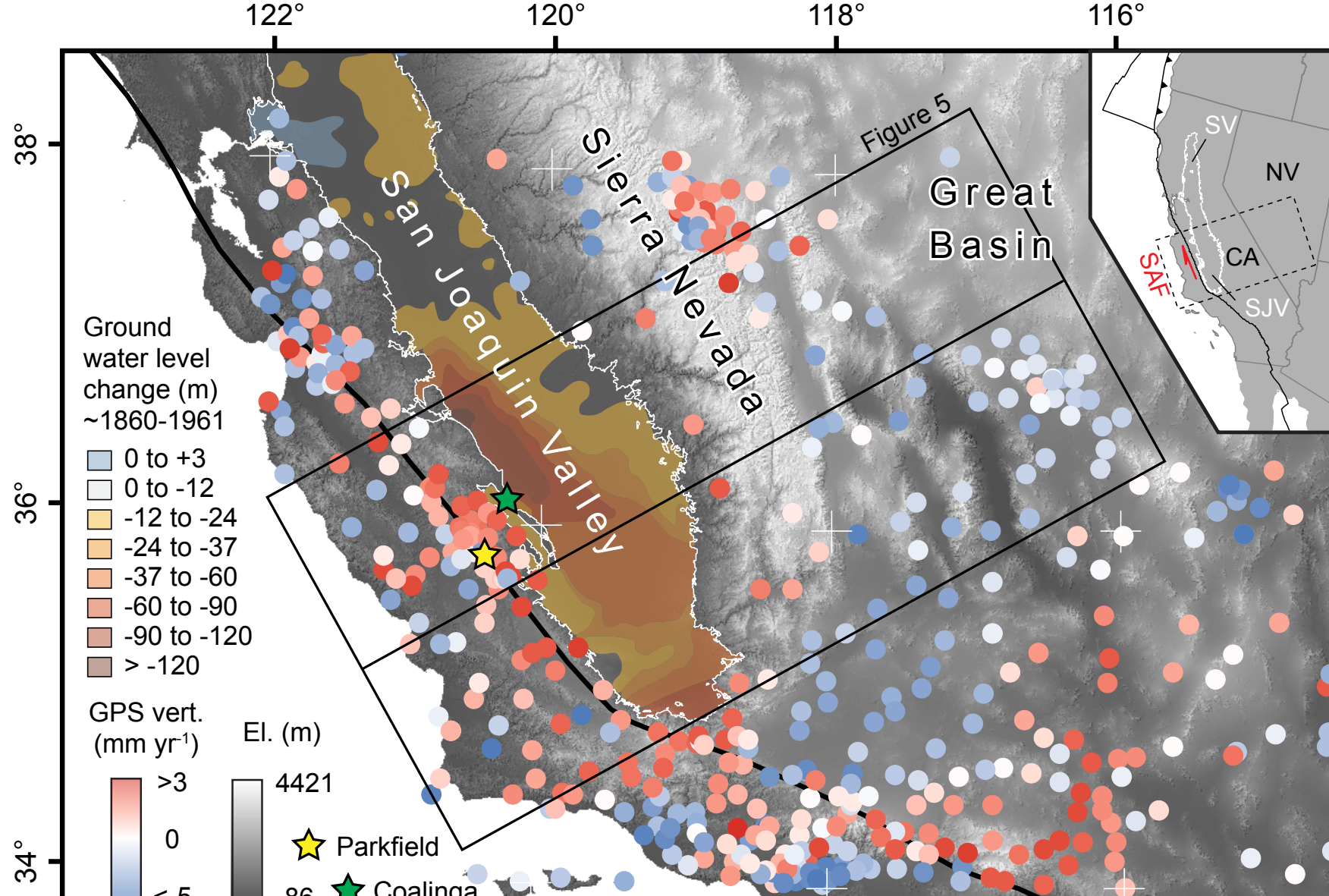


Figure 3. | Contemporary GPS vertical rates and groundwater decline.

Map of vertical GPS uplift rates, excluding stations in the SJV showing anomalously larger signals and local irrigation effects. Contours show historical changes in the deep, confined aquifer¹.

(SV – Sacramento Valley, SJV – San Joaquin Valley), and the San Andreas Fault (SAF).

Recent groundwater loss estimated from GRACE data³:

Total water storage = $30.9 (\pm 2.6) \text{ km}^3$ (October 2003 through March 2010)

Central Valley groundwater = $20.3 (\pm 3.8) \text{ km}^3$, 80% of which occurred in the San Joaquin Valley^{2,3}.

Historical groundwater change:

~160 km³ of groundwater lost between 1860-2010 (refs. 2, 3)

4. Elastic Unloading Model

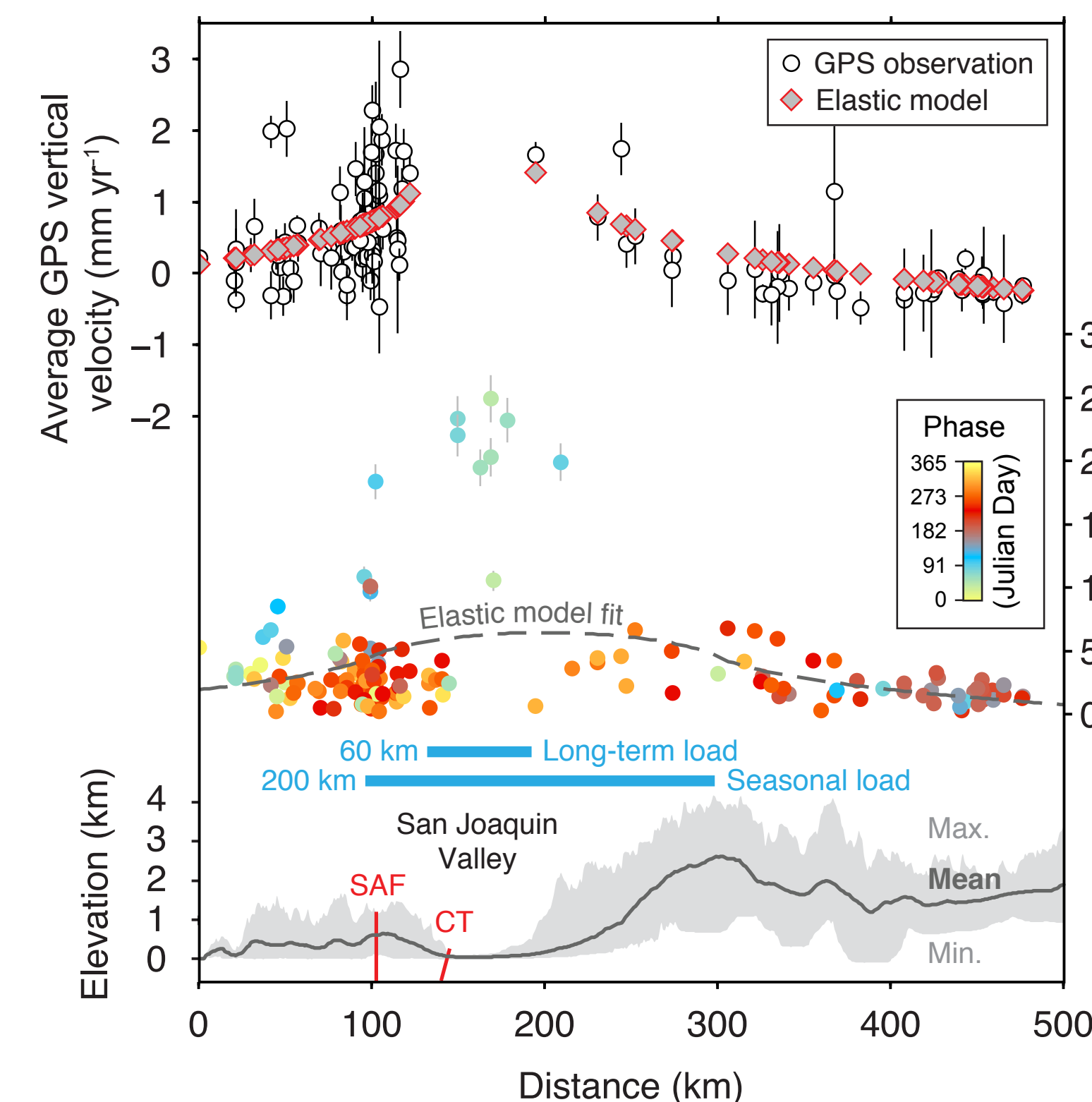


Figure 4. | GPS and 2D line-load model comparison.

Swath profile of average contemporary vertical GPS velocity (top), annual GPS vertical displacement (middle), and average topography from the central California Coast Range to the western Great Basin (SAF – San Andreas Fault, CT – Coalinga thrust) (bottom). Blue bars show the width of both long-term and seasonal loads used in the elastic model.

2D line-load along San Joaquin Valley

Calculated unloading rate from GPS data and estimates of recent groundwater loss from GRACE data.

Unloading rates:

Elastic model
 $8.8 (\pm 1.3) \times 10^7 \text{ N m}^{-1} \text{ yr}^{-1}$
GRACE mass loss
 $7.2 (\pm 2.1) \times 10^7 \text{ N m}^{-1} \text{ yr}^{-1}$

Seasonal uplift due to yearly change in total water storage distributed across entire basin. Displacement is calculated as twice the seasonal amplitude.

5. Seasonal Stress Changes and Seismicity

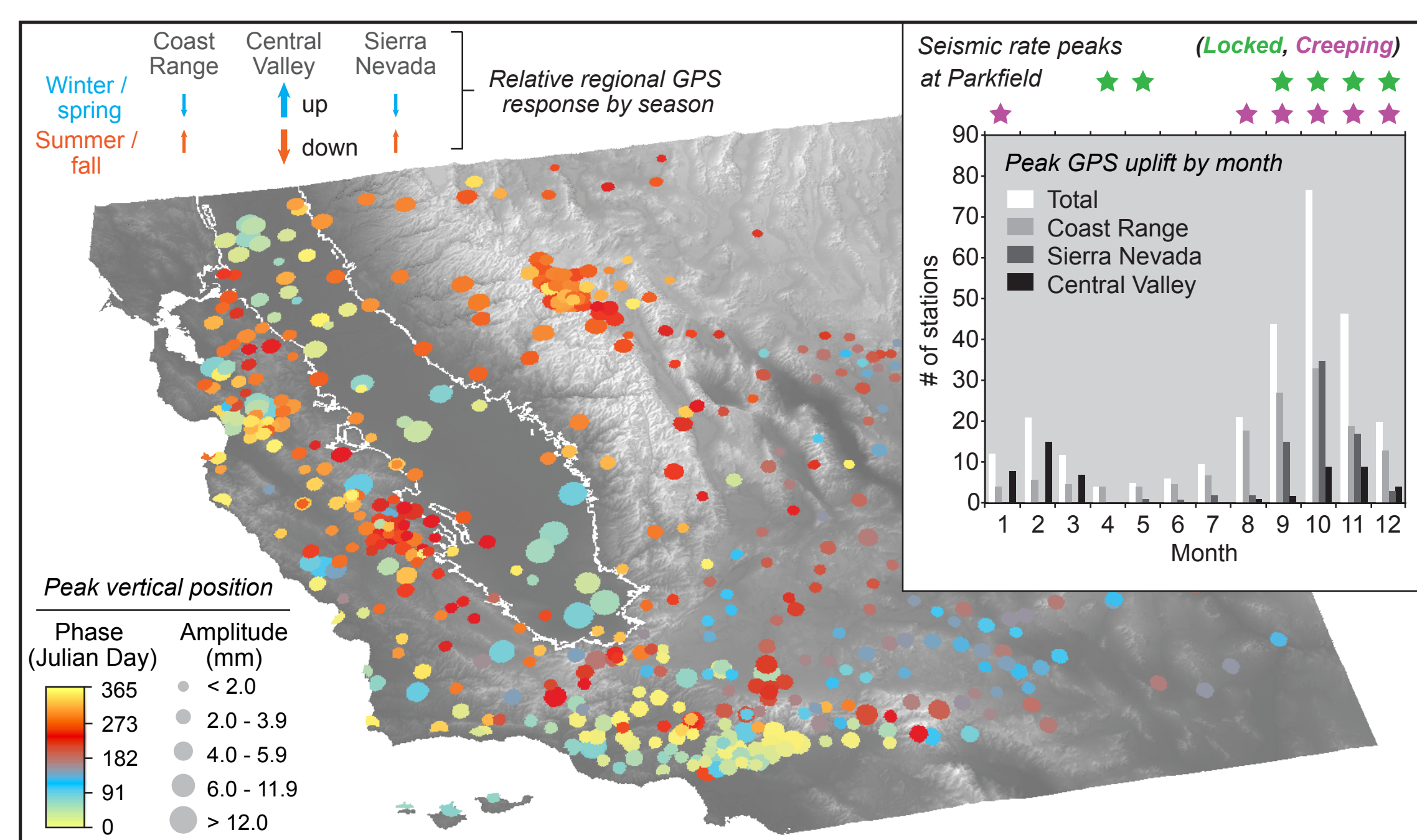
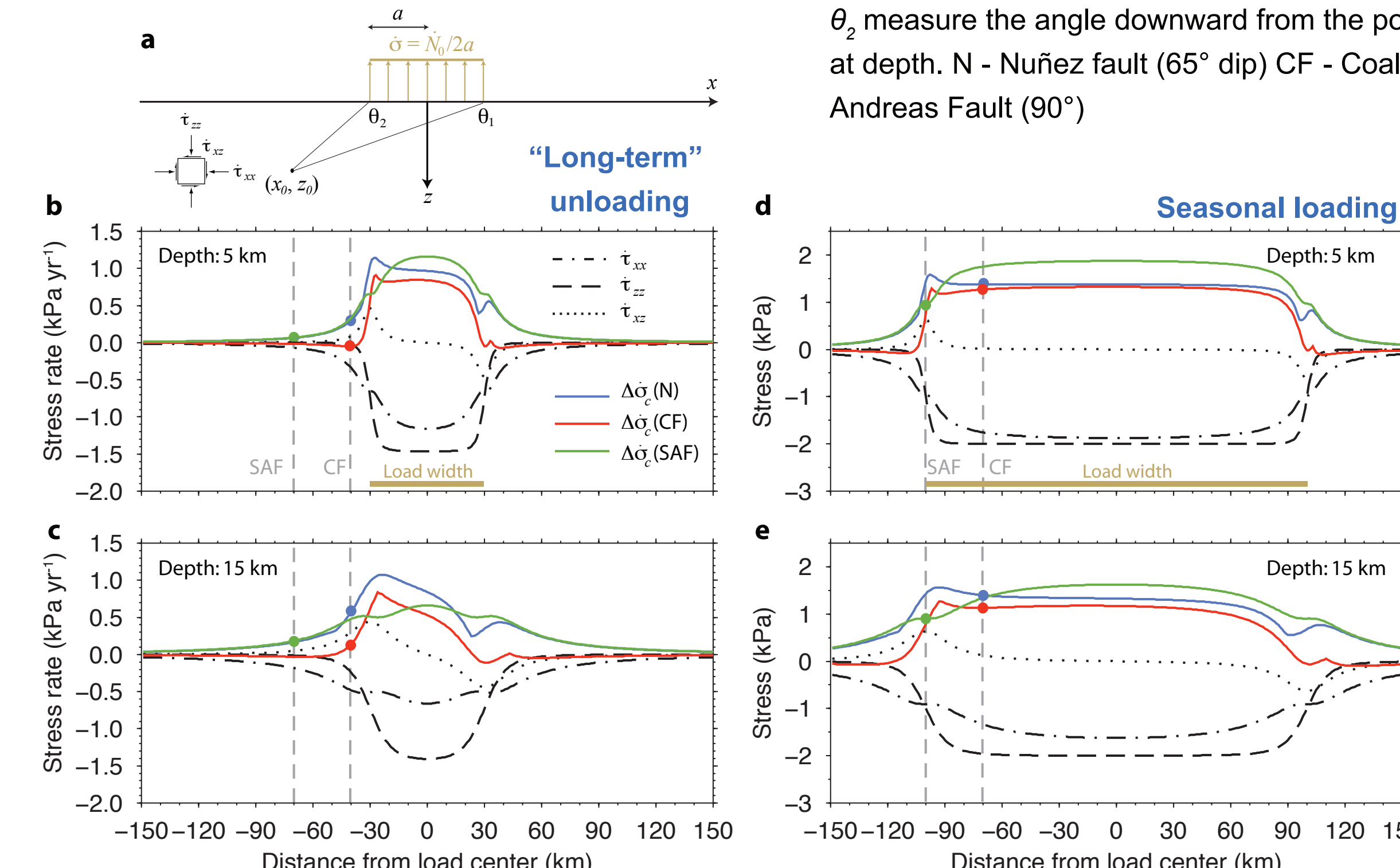


Figure 5. | Seasonal peak uplift from GPS.

Phase and peak-to-peak amplitude of annual vertical GPS displacement for all stations included in our analysis. Inset shows histograms of peak uplift phase (binned by month) for stations in the SJV, Sierra Nevada, and Coast Range. Peaks in seismicity rate for the locked and creeping San Andreas Fault at Parkfield are defined as months with higher than average declustered seismicity⁴.

Figure 6. | Stress changes over an elastic half-space



Model setup (top) N = line load, a = load half-width (here 30 km), and θ_1 and θ_2 measure the angle downward from the positive x-axis to any point (x_0, z_0) at depth. N - Nuñez fault (65° dip) CF - Coalinga fault (15, 30°) SAF - San Andreas Fault (90°)

Seasonal changes at 5 - 15 km
(~200 mm of water height change)

SAF = $\sim 1.0 \text{ kPa } (\Delta\sigma_n)$
CF = $\sim 1.0 - 1.7 \text{ kPa } (\Delta\sigma_c)$

"Long-term" unclamping rate:

SAF = $\sim 0.07 - 0.18 \text{ kPa yr}^{-1} (\Delta\sigma_n)$,
 $\sim 2.7 - 9.5 \text{ kPa}$ since 1860
CF = $\sim 0.13 - 0.57 \text{ kPa yr}^{-1} (\Delta\sigma_c)$,
 $\sim 10 - 15 \text{ kPa total}$

6. Conclusions

1. GPS uplift is well-matched by elastic model simulating groundwater unloading.
2. Seasonal uplift in the Coast Range corresponds with seismic rate peaks.
3. Contemporary uplift of Sierra Nevada may reflect human-caused hydrospheric change
4. Induced stress changes may contribute to seasonal modulation of seismicity.

For more, see: Amos et al., 2014, *Nature*, 509, doi:10.1038/nature13275

References:

1. Williamson, A. K., Prudic, D. E. & Swain, L. A. *USGS Prof. Paper*, 1401 (1989).
2. Scanlon, B. R. et al. *PHAS* 109, (2012).
3. Famiglietti, J. S. et al. *GRL*, 38, (2011).
4. Christiansen, L. B., Hurwitz, S. & Ingebritsen, S. E. *GRL*, 34, (2007).

Acknowledgements:

Funding: NSF EarthScope award number EAR-1252210 to G.B. and W.C.H. GPS data: EarthScope Plate Boundary Observatory, SCIGN, BARGEN, BARD, CORS and IGS networks. We are particularly grateful to UNAVCO for operating the vast majority of GPS stations used in this project.